British Journal of Applied Science & Technology
13(3): 1-14, 2016, Article no.BJAST.22578
ISSN: 2231-0843, NLM ID: 101664541

SCIENCEDOMAIN *international*
www.sciencedomain.org

Fluid-Structure Interaction and Aeroelastic Balance on the Analysis of a Tall Building with Irregular Geometry

J. M. Horta-Rangel[1*], J. P. Lara-López[1], J. G. Valdés-Vázquez[2] and I. Arreola-Sifuentes[3]

[1]Department of Graduate Engineering, Universidad Autonoma de Queretaro, Cerro de las Campanas s/n Querétaro, Qro. C. P. 76010, Mexico.
[2]Department of Civil Engineering, Universidad de Guanajuato, Ave. Juárez 77 Guanajuato, Gto. C. P. 36000, Mexico.
[3]Design Lab Constructions, Laguna Norte 236, Torreon, Coah. C. P. 27000, Mexico.

Authors' contributions

This work was carried out in collaboration between all authors. Author JMHR designed the study, managed the scope of numerical and experimental analysis, revised the manuscript. Author JPLL conducted and realized the numerical calculations as well the experimental tests, wrote the first draft of the manuscript and managed literature searches. Author JGVV conducted the numerical tests on Dines+Gid and revised the manuscript. Author IAS conducted the experimental test on wind tunel. All authors read and approved the final manuscript.

Article Information

DOI: 10.9734/BJAST/2016/22578
Editor(s):
(1) Jakub Kostecki, Department of Civil and Environmental Engineering, University of Zielona Góra, Poland.
Reviewers:
(1) Fuad Okay, Kocaeli University, Turkey.
(2) Tian- Quan Yun, South China University of Technology, China.
Complete Peer review History: http://sciencedomain.org/review-history/12417

Original Research Article

Received 12th October 2015
Accepted 2nd November 2015
Published 25th November 2015

ABSTRACT

Aims: In this work the effect of wind on a building with irregular geometry is analyzed. Today, many cases of computational fluid-structure phenomena are validated with Benchmark models; nevertheless, the structure analyzed in this work does not have an associated benchmark model. Numerical algorithms applied in this work are also validated with a physical scale model under wind loads on a subsonic wind tunnel.
Study Design: Developed procedure involves two coupled field models corresponding to fluid and mechanical phenomenology, each one governed by different methodology: Fluid field associates

**Corresponding author: E-mail: horta@uaq.mx;*

an Eulerian Configuration, meanwhile solid model is described on Lagrangean configuration. These two models require a third model named ALE to interact each other; this last model is built on the interfaces between them. This work develops the numerical procedure as well experimental ones for solving these complex structures.
Place and Duration of Study: Graduate Engineering Lab. Universidad Autonoma de Queretaro, Mex., Civil Engineering Department. Universidad de Guanajuato, Mex., Design Lab. Construction, Torreon Cohauila, Mex., between September 2012 and July 2014.
Methodology: The numerical model was analyzed through the software ANSYS and also DINES + GiD while the experimental test was performed in a subsonic wind tunnel. The prototype consists of structural steel sections while walls are made of glass panels; physical model belongs to an elastic model where the effect of twisting is not included.
Results: Main results obtained in this work are the bending moment at the basement of the building, the displacement at the top of the structure and the non-uniform pressure distribution on the structural walls.
Conclusion: Dynamic fluid-structure interaction (IDFE) problems have attracted the attention of a large number of researchers. IDFE plays an important role in the structural engineering: on the analysis of high-rise buildings, large bridges, industrial plants, chimneys, transmission towers, etc., all these structures may collapse due to the aeroelastic instability caused by wind effect. The goal of this work is provide a methodology for real structures of complex geometry.

Keywords: Fluid-structure interaction; structural dynamics; coupled fields; aeroelastic modeling.

1. INTRODUCTION

In recent years various scientific areas have had an important development, one of the areas where an important progress has been seen on the analysis of dynamic fluid-structure interaction (IDFE) problems which has attracted the attention of a large number of researchers [1-3]. The IDFE studies play an important role in the structural engineering as on the analysis of high-rise buildings, large bridges, industrial plants, chimneys, transmission towers, etc., all these structures may collapse due to the aeroelastic instability caused by wind effect [4,5]. The complexity of this phenomenology leads to research on experimental procedures (usually in wind tunnels) as well in numerical algorithms through computational fluid dynamics (CFD), taking this into account, two groups of research are clear, the first one addressed to obtain the maximum effects of wind occurring in the structure, while the second focuses on the evaluation of maximum flow effects [6].

These kinds of problems are treated as coupled models [7], they are multi-physical problems governed by phenomenologies interacting simultaneously [8], Most researchers consider IDFE phenomenology as a case including three main fields: solid (structural), fluid (wind) and interface (border) between domains [5]. The solution of these cases keeps some difficulty because the total domain has to be divided into structural subdomain as well as fluid subdomain which associate different configurations: Lagrangian and Eulerian ones, which are not compatible each other [9]. Therefore generated geometries tend to be complex, whereas the boundary conditions between fluid and structure are nonlinear due to movements of the interface, besides, the position of the interface is part of the solution [10,11].

The key for solving these problems is a method consisting of coupling these two phenomenologies: structural and fluid dynamics, in addition it must be included movement techniques of nonstructural meshes for the fluids in order to represent the movement of the interface. It is also required stabilization methods and segregation of pressures for the fluid domain as well a block method for solving the coupling, all this together with computational procedure for large scale solutions [12].

Related to experimental tests in wind tunnels, the aeroelastic "stick" model is popular for its efficiency in the design, manufacture, calibration and measurement procedures. In most structures under wind effects has been observed that the fundamental modes of vibration are the most significant, this feature promotes simplification of the "stick" model by which only two fundamental modes of translation is enough to include for obtaining a direct similarity between the model and prototype structure [13].

2. MATERIALS AND METHODS

2.1 Phenomenological Continuum Equations

The equilibrium equation of a continuous medium is given by the following relation (1), while equation of local mass conservation is expressed by the relation (2), [14]:

$$\operatorname{div}\mathbf{T}+\mathbf{b}=\rho\dot{\mathbf{v}} \tag{1}$$

$$\rho^{'}+\operatorname{div}(\rho\mathbf{v})=0 \tag{2}$$

T is the Cauchy stress tensor, b is the body force field, ρ density field, velocity field v. Moreover, the constitutive equation for a Newtonian fluid is expressed by the next relationship:

$$\mathbf{T}=-\pi\mathbf{I}+2\mu\mathbf{D} \tag{3}$$

here π pressure is a scalar field, D is the spatial gradient tensor of velocity, μ is the viscosity fluid and I is a identity tensor. Substituting equation (3) in (1) and (2) the Navier-Stokes equation for a Newtonian fluid are obtained:

$$\rho\left[\mathbf{v}^{'}+(\operatorname{grad}\mathbf{v})\,\mathbf{v}\right]=-\operatorname{grad}\pi+\mu\Delta\mathbf{v}+\mathbf{b} \tag{4}$$

$$\operatorname{div}\mathbf{v}=0 \tag{5}$$

On the other hand, the constitutive equation of a homogeneous isotropic elastic solid is given by the equation:

$$\mathbf{S}=2\mu\mathbf{E}+\lambda(\operatorname{tr}\mathbf{E})\mathbf{I} \tag{6}$$

where E is the tensor of infinitesimal deformation, λ and μ are Lame constants.

2.2 Dynamic Models

2.2.1 Solid

The matrix equation governing the dynamic behavior of a solid is given by the following equation [15]:

$$[\mathbf{M}]\ddot{\mathbf{u}}+[\mathbf{C}]\dot{\mathbf{u}}+[\mathbf{K}]\mathbf{u}=\mathbf{F_b}+\mathbf{F_t} \tag{7}$$

Being $[\mathrm{M}],[\mathrm{C}]\ \text{and}\ [\mathrm{K}]$ mass, damping and stiffness matrices respectively, also u, $\dot{\mathrm{u}}$, $\ddot{\mathrm{u}}, \mathrm{F_b}\ \text{and}\ \mathrm{F_t}$ are the vectors of displacement, velocity, and acceleration in addition to the force vectors and surface forces respectively, the latter ones commonly as a time-dependent vector. This equation (7) associates a set of linear or nonlinear equations depending on the structure of the matrix involved in the process. A typical solution of (7) is given by the method of Newmark where displacement and velocity fields are approximated by the following relationships [4,15]:

$$\mathbf{u}(t)^{\mathrm{n}+1}=\mathbf{u}^{\mathrm{n}}+\dot{\mathbf{u}}^{\mathrm{n}}\Delta t+\left[\left(\tfrac{1}{2}-\beta\right)\ddot{\mathbf{u}}^{\mathrm{n}}+\beta\ddot{\mathbf{u}}^{\mathrm{n}+1}\right]\Delta t^{2} \tag{8}$$

$$\dot{\mathbf{u}}\,(t)^{\mathrm{n}+1}=\dot{\mathbf{u}}^{\mathrm{n}}+[(1-\gamma)\ddot{\mathbf{u}}^{\mathrm{n}}+\gamma\ddot{\mathbf{u}}^{\mathrm{n}+1}]\Delta t \tag{9}$$

β and γ are parameters of stability of the method, Δt is the time step [16,17].

2.2.2 Fluid

Analogously, the discrete equations governing the behavior of the fluid are described below:

$$[\mathbf{M}]\,\ddot{\mathbf{u}}+[\mathbf{K}]_{\dot{\mathrm{u}}}(\dot{\mathrm{u}})\dot{\mathbf{u}}-[\mathbf{G}]\mathbf{p}+[\mathbf{K}]_{\mu}\dot{\mathbf{u}}=\mathbf{F_b}+\mathbf{F_t} \tag{10}$$

$$[\mathbf{G}]^{\mathrm{T}}\dot{\mathbf{u}}=0 \tag{11}$$

Here $[\mathrm{M}]$, $[\mathrm{K}]_{\dot{\mathrm{u}}}$, $[\mathrm{G}]$, $[\mathrm{K}]_{\mu}$ represent the mass, convection, pressure and viscosity matrix respectively, $\dot{\mathrm{u}},\ddot{\mathrm{u}},\mathrm{p},\mathrm{F_b}\ \text{and}\ \mathrm{F_t}$ are the velocity, acceleration, pressure, body forces and surface force vector respectively. Equations (10) and (11) are a set of nonlinear equations. The solution of these equations is based on the implicit integration scheme of Euler [5,18]:

$$[\mathbf{M}]\left[\frac{3\dot{\mathbf{u}}_{\mathrm{n}+1}-4\dot{\mathbf{u}}_{\mathrm{n}}+\dot{\mathbf{u}}_{\mathrm{n}-1}}{2\Delta t}\right]+[\mathbf{K}](\cdot)[\dot{\mathbf{u}}_{\mathrm{n}+1}]-[\mathbf{G}]\mathbf{p}_{\mathrm{n}+1}=\mathbf{F}_{\mathrm{n}+1} \tag{12}$$

$$[\mathbf{G}]^{\mathrm{T}}\dot{\mathbf{u}}_{\mathrm{n}+1}=0 \tag{13}$$

The process of solving of the discrete model described in these equations (12) and (13) requires a method of stabilization, particularly Ansys program uses SUPG (Streamline-upwind/Petrov–Galerkin) and PSPG (Pressure stabilized/Petrov–Galerkin) [19], whose methodology is based on the following equation:

$$\int_{\Omega}\left[\mathbf{N}+\boldsymbol{\delta}^{\mathrm{h}}+\boldsymbol{\varepsilon}^{\mathrm{h}}\right]^{\mathrm{T}}(\rho[\mathbf{v}'+(\operatorname{grad}\mathbf{v})\mathbf{v}]+\operatorname{grad}\pi-\mu\Delta\mathbf{v}-\mathbf{b}+\operatorname{div}\mathbf{v})\mathrm{d}\Omega=0 \tag{14}$$

The terms $\boldsymbol{\delta}^{\mathrm{h}}\ \text{and}\ \boldsymbol{\varepsilon}^{\mathrm{h}}$ are the stabilizers terms called SUPG y PSPG, The latter equation (14) is solved using the scheme named "SIMPLE" (semi-implicit method pressure linked equations) where grades of freedom corresponding to the velocity are solved with the algorithm "TDMA" (tri-diagonal matrix algorithm) and the pressure

are solved with the method of residual conjugate pre-conditioned. The integration process (14) is quite similar to that indicated in the equations (10) and (11). In contrast, the DINES + GiD software uses the stabilization method OSS (orthogonal sub-scale) expressed by the relation [5,20]:

$$[\mathbf{M}]\ddot{\mathbf{u}} + [\mathbf{K}]_{\dot{u}}(\dot{u})\dot{\mathbf{u}} + [\mathbf{K}]_{\mu}\dot{\mathbf{u}} - [\mathbf{G}]\mathbf{p} + [\mathbf{G}]^{\mathrm{T}}\dot{\mathbf{u}} + \boldsymbol{\tau}(\cdot) = \mathbf{F_b} + \mathbf{F_t} \quad (15)$$

Here τ(·) is the stabilization parameter described in [5], then a fractional step scheme is used. The key is to use the auxiliary variable u˙and the following approximation [21]:

$$\mathbf{K}(\cdot)[\dot{\mathbf{u}}_{n+1}] \approx \mathbf{K}(\cdot)\left[\tilde{\dot{\mathbf{u}}}_{n+1}\right] \quad (16)$$

Thus, equations (12) and (13) are transformed into the following equivalent relationship:

$$[\mathbf{M}]\left[\frac{3\dot{\tilde{\mathbf{u}}}_{n+1} - 4\dot{\mathbf{u}}_n + \dot{\mathbf{u}}_{n-1}}{2\Delta t}\right] + [\mathbf{K}](\cdot)\left[\tilde{\dot{\mathbf{u}}}_{n+1}\right] - [\mathbf{G}]\mathbf{p}_n + \mathbf{E_1} = \mathbf{F}_{n+1} \quad (17)$$

$$-\frac{2}{3}\Delta t\,[\mathbf{G}]^{\mathrm{T}}\,[\mathbf{M}]^{-1}\,[\mathbf{G}](\mathbf{p}_{n+1} - \mathbf{p}_n) + \mathbf{E_2} = [\mathbf{G}]^{\mathrm{T}}\tilde{\dot{\mathbf{u}}}_{n+1} \quad (18)$$

$$[\mathbf{M}]\left[\frac{3\dot{\mathbf{u}}_{n+1} - 3\dot{\tilde{\mathbf{u}}}_{n+1}}{2\Delta t}\right] - [\mathbf{G}](\mathbf{p}_{n+1} - \mathbf{p}_n) = 0 \quad (19)$$

Where E_1 and E_2 are stabilizers terms of the OSS scheme corresponding to the momentum and continuity equations respectively. The resulting equations from this methodology of fractional steps are solved by the method of Picard.

2.3 Coupled Model

In previous pages the structural and fluid models were raised in its Lagrangian and Eulerian domain respectively, however, when considering the interaction between these domains, incompatibilities can be solved through a third description called ALE (Algorithm Lagrangian Eulerian) [22]. This procedure refers a mesh movement method complying the law of geometric conservation, there are several methods of moving mesh, one of the most used is the Laplacian method [8,23]:

$$\Delta\mathbf{u}_{\mathrm{m}} = 0 \quad (20)$$

u_{m} is the movement of mesh nodes in areas near of the structural domain. As the nodes of the mesh of the fluid domain can move arbitrarily, is necessary then to consider the convective velocity c defined by [24]:

$$\mathbf{c} = \mathbf{v} - \bar{\mathbf{v}} \quad (21)$$

Being v and $\bar{\mathrm{v}}$ the material flow velocity and the velocity of the mesh respectively, therefore, considering (21) is obtained the following equation [5]:

$$[\mathbf{M}]\ \ddot{\mathrm{u}} + [\mathbf{K}]_{\dot{u}}(\dot{u})\mathbf{c} - [\mathbf{G}]\mathbf{p} + [\mathbf{K}]_{\mu}\dot{\mathbf{u}} - \mathbf{F} + [\mathbf{G}]^{\mathrm{T}}\dot{\mathbf{u}} + \Delta\mathbf{u}_{\mathrm{m}} + \mathbf{E_1} + \mathbf{E_2} = 0 \quad (22)$$

which is the set of discrete equations on the domain of the fluid. The integration procedure for this equation (22) is similar to the equations of fluid mechanics indicated above. Mesh movement is considered only in the vicinity of fluid domain with the structural domain. Similarly, equation (11) is modified as follows:

$$[\mathrm{M}]\ddot{\mathrm{u}} + [\mathrm{C}]\dot{\mathrm{u}} + [\mathrm{K}]\mathrm{u} = \mathrm{F_b} + \mathrm{F_t} + \mathrm{H} \quad (23)$$

Here H is the effect of the fluid domain over the structural domain. Boundary kinematics and dynamics conditions required in the solution of the coupled problem are indicated as follows:

$$\mathrm{x}_0^s + \mathrm{d} = \mathrm{x}\ ,\quad \dot{\mathrm{d}} = \mathrm{u} \quad (24)$$

$$\mathrm{Tn} = \mathrm{Sn} \quad (25)$$

Where d is the structural displacement during the interaction, x_0^s is the initial position of the structural domain and n is a unit normal vector. The equation (22) and (23) are solved by the block method Gauss-Seidel [25]:

$$\mathbf{x}_{k+1}^{n+1} = \mathrm{F}(\mathbf{x}_k^n, \mathbf{y}^n) \quad (26)$$

$$\mathbf{y}_{k+1}^{n+1} = \mathrm{E}(\mathbf{x}^{n+1}, \mathbf{y}_k^n) \quad (27)$$

F and E are abstract representations of equations (22) and (23) respectively, x and y are the unknowns of fluid domains (velocity and pressure) and structural (displacement), n represents the time step and k is a counter for controlling the iterations sets.

2.4 Experimental Procedure

2.4.1 Aeroelastic balance

When considering the effect of Aeroelastic Structure, we can rewrite equation (7) as follows [13,26]:

$$m\ddot{\mathrm{u}} + c\dot{\mathrm{u}} + k\mathrm{u} = \mathrm{F}(t, \mathrm{u}, \dot{\mathrm{u}}, \ddot{\mathrm{u}}) \quad (28)$$

where the force vector F is a function of time, movement and its derivatives. The form of the first mode of vibration of the structure to be analyzed can be approximated by the following exponential equation [13]:

$$\varphi(\mathbf{z}) = \alpha \left(\frac{\mathbf{z}}{H}\right)^{\beta} \quad (29)$$

α and and β are normalization coefficients, H is the total height of the structure z is a height between H and zero. For a linear mode shape, considering scaling laws described in [13,27], together with relation (28), and according to [16,28] we obtain:

$$\ddot{\mathbf{u}} + \left(\frac{1}{K_\zeta}\right) 4\pi f_m \dot{\mathbf{u}} + (2\pi f_m)^2 \mathbf{u} = \frac{M_m/H_m}{m_m}\left(\frac{1}{K_{CM}}\right)\left(\frac{1}{K_{\rho_a}}\frac{K_\rho}{K_L{}^3}\right)\left(\frac{K_L}{K_t K_V}\right) \quad (30)$$

Here f_m the fundamental frequency in the wind direction, M_m is the bending moment at the basement, H_m is the total height of the structure, the subindex m indicates that these three parameters are related to the physical scale model. Equation (30) refers the scaling laws regarding damping, force coefficient, generalized mass and stiffness. These scaling laws are functions of $K_L, K_V, K_t, K_{CM}, K_{\rho_a}, K_\rho$ and K_ζ representing geometry similarities, wind velocity, frequency, force coefficient, density, mass and damping between the physical scale model and the prototype [13].

Based on these scaling laws, the model represents a direct similarity with the prototype and can be obtained the bending moment at the basement of the scale model as well as the displacement at any point in the model. The ratio between the bending moment at the basement for the model and the prototype is K_M and it is defined by [13]:

$$K_M = \frac{k_{\rho a}\, K_L{}^5}{k_t{}^2} \quad (31)$$

2.4.2 Wind tunnel settings

The mass of the physical model is obtained by applying equation [13]:

$$m(\mathbf{z})_i = \frac{m_{pi}(K_{\rho a})(K_L)^3}{\varphi^2{}_i} \quad (32)$$

m_{pi} is the general mass of prototype and φ the fundamental mode shape in the wind direction. Once the model was built, its damping is determined by the logarithmic decrement method [28]:

$$\xi = \sqrt{\frac{\delta^2}{4\pi^2+\delta^2}} \quad (33)$$

Where δ is the logarithmic decrement and ξ the damping factor. After built the Physical model, its fundamental frequency f_{1m}. Wind velocity in the tunnel is determined by the following relationship:

$$v_m = (K_L)\left(\frac{1}{K_t}\right) v_p \quad (34)$$

v_m and v_p are the wind velocity applied to the model (on the wind tunnel) and the corresponding velocity of the prototype. Before making the measurements in the wind tunnel is required to establish a calibration equation based on the displacement of the model resulting of a known force and its point of application, this same equation will be applied to the measurements on the wind tunnel with the difference that the force will be produced by the wind. The moment of the prototype is given by the equation (31):

$$M_p = M_m \frac{(K_t)^2}{(K_L)^5} \quad (35)$$

M_p and M_m are the bending moment at the basement of the prototype and the model respectively, in (35) has been considered that the air density in the model and prototype are identical.

2.5 Test Models

2.5.1 Properties

The structural prototype has a prismatic shape depending on the height, the structural elements are made of steel and concrete, the building is covered with glass plates to prevent the flow of wind inside (Fig. 1). The total height is 72.0 meters, it has 18 slabs (including the roof one) uniformly spaced. Table 1 shows the mechanical properties of the prototype applied in this work while in Table 2 are shown the geometrical properties of the structural sections. Numerical models were developed in ANSYS [29], and DINES + GiD [30,31] software and the experimental test was carried out on a subsonic wind tunnel.

All beams are sections W18x35, all levels to a height of 12.00 meters are supported with columns HSS16, next levels up to a height of 24.00 meters are supported by columns HSS14, the following levels to a height of 48.00 meters are HSS12 columns sections, the rest of the levels are supported by columns sections HSS10. The slab and glass sections are identical in all levels. Each column-column connections and beam-column are rigid type. All supports at basement of building have been considered fixed.

Table 1. Mechanical properties

Material	E (N/m^2)	v (-)	ρ(kg/m^3)	μ (kg/m^2 s)
Steel	2.00x10^{11}	0.250	7,800	-
Concrete	2.25x10^{10}	0.100	2,400	-
Glass	1.00x10^{1}*	0.225	0.500	
Wind	-	-	1.185	1.831x10^{-5}

Table 2. Structural sections

Section	d (m)	b (m)	t_f (m)	t_w (m)
W18x35	0.4496	0.1524	0.0108	0.0076
HSS16	0.4064	0.4064	0.0127	-
HSS14	0.3556	0.3556	0.0127	-
HSS12	0.3048	0.3048	0.0127	-
HSS10	0.2540	0.2540	0.0127	-
Slab	0.1100	-	-	-
Glass	0.0050	-	-	-

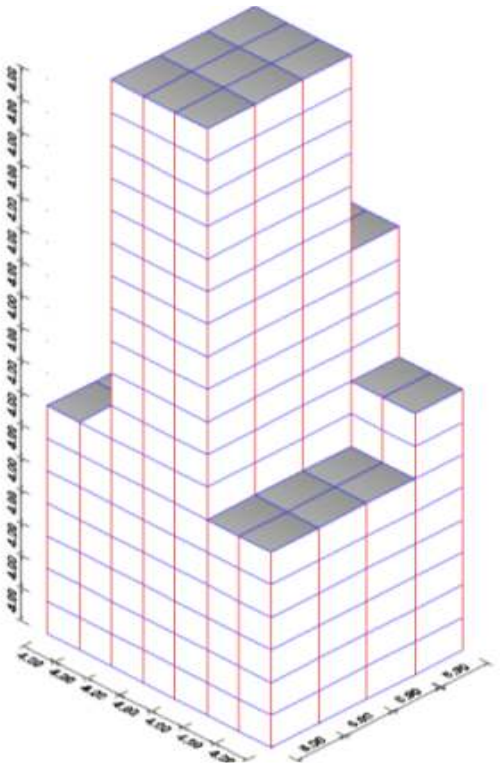

Fig. 1. Main dimensions of the Irregular Building composed of steel structure and reinforced concrete slabs

The domain of the fluid surrounds the structural domain is shown on Fig. 2, the fluid domain size and boundary conditions considered in this work are indicated. In all areas dividing the two domains is considered a velocity v = 0 m / s. The hatched area on Fig. 2 shows the structural domain.

2.5.2 Computational modeling in ansys

The discrete model was built with 50,228 finite elements. For beams and columns have been used elements "beam" with 6 degrees of freedom per node. For concrete slabs as well as cover glass on windows have been used elements "shell" with 12 degrees of freedom (see Fig 3). To model the fluid, finite elements "brick" of 24 degrees of freedom were used. The structural model solution obeys the equation (23) with β = 1/6 and γ = 1/2. The fluid domain use equations (12), (13), (14), (22), while coupling of fields applied equations (20), (26) and (27). In both domains was used a step time of 0.01 seconds, having carried out a total of 500 iterations, the convergence criteria used for displacements was 1x10^{-3}, whereas in velocities 1x10^{-6} and for pressures 1x10^{-3}. Figs. 3(a) and 3(b) show the internal structure geometry together with elements "beam" and "shell". Fig. 3(c) shows the external geometry of the structure including the domain of fluid that surrounds the structural domain.

2.5.3 Computational modeling with DINES + GiD

In this case only was modeling the fluid domain, structural domain has been considered as a rigid body. A total of 113.000 finite elements were required. The fluid was modeled with elements "brick" of 24 degrees of freedom. Fluid domain was solved by equations (12), (13), (15), (17), (18), (19), and (22). The time step used was 0.01 seconds, 1,000 iterations in total were performed, and the convergence criteria were in velocities equal to 1x10^{-6} while in pressures

$1x10^{-3}$. Fig. 4 shows the domain of the fluid which surrounds the structural domain.

2.6 Test on Wind Tunnel

The fundamental frequency of the building in wind direction was initially determined turning out to be 0.51 Hz and the mode shape associated as shown in Fig. 5. The scale model (Fig. 6) was made with PVC foamed material and scaled from the first fundamental vibration mode. The prototype analyzed has not a linear mode shape, however, in this work was linear considered taking parameters $\alpha = 1.00$ and $\beta = 0.914$ according to (29). In Fig. 5 are shown both modes.

Considering the fundamental linear mode in (32) and a geometric scale 1: 200 it has been obtained a mass scale model of 0.293 kg (while the prototype has a mass of 2345 $x10^3$ kg). Using equation (33) we obtain a damping factor of 0.0418, this value was also used in ANSYS modeling. The frequency of the model was obtained experimentally proving to be of 20.81 Hz, and by means of equation (34) has been obtained the wind velocity inside the tunnel of 11.11 m / s. Equipment used for physical experimentation is shown in Figs. 7 and 8. Table 3 shows a comparison between the physical parameters of the model and prototype used.

3. RESULTS AND DISCUSSION

The model inside the wind tunnel was instrumented in wind direction; hence the results that will be validated with the numerical results will be only the ones corresponding to this direction. On the other hand, the bending moment at the basement obtained with Ansys [29] was 47.504 kN-m with a displacement at the top of 0.936 meters in a time of 1.30 seconds. Figs. 9 and 10 show some of the numerical results obtained with Ansys.

Through Dines + Gid software [30,31], it has been obtained at the Building basement a bending moment of 53.706 kN-m in a time of 1.06 seconds. Figs. 11-12 show some results corresponding to the pressure generated by the bending moment at the basement.

In the wind tunnel the bending moment at the basement of the model was obtained as 0.291 Nm and a displacement at the top of model of 0.00458 meters. Applying the scale law (35) and considering a geometrical scale 1: 200 the bending moment at the basement of prototype will be 55,397 kN-m while the corresponding displacement at the top of the building of 0.916 meters.

Table 3. Physical parameters

Parameter	Model	Prototype
Mass (kg)	0.293	$2{,}345x10^3$
Height (m)	0.36	72.0
Period (s)	0.048	1.96
Frequency (Hz)	20.81	0.51
Damping (-)	0.0418	0.0418
Wind velocity (m/s)	11.11	55.0

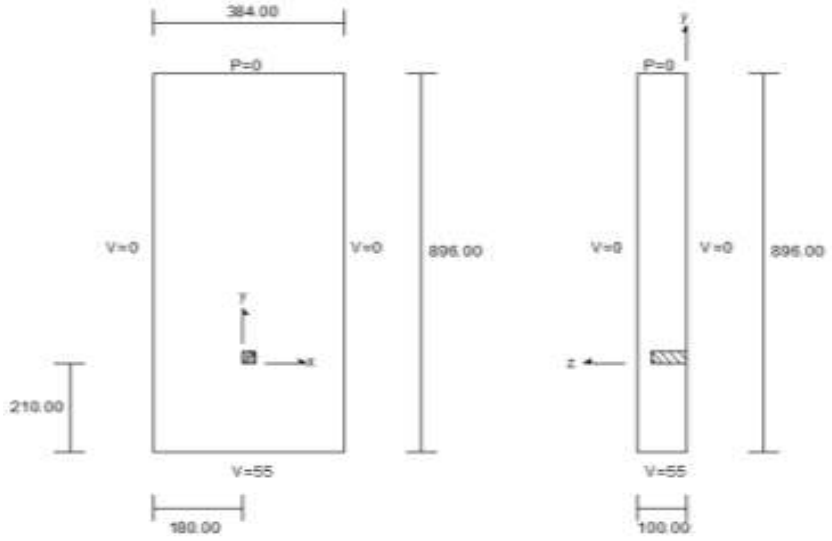

Fig. 2. Domain fluid on planes "xy" and "yz" respectively

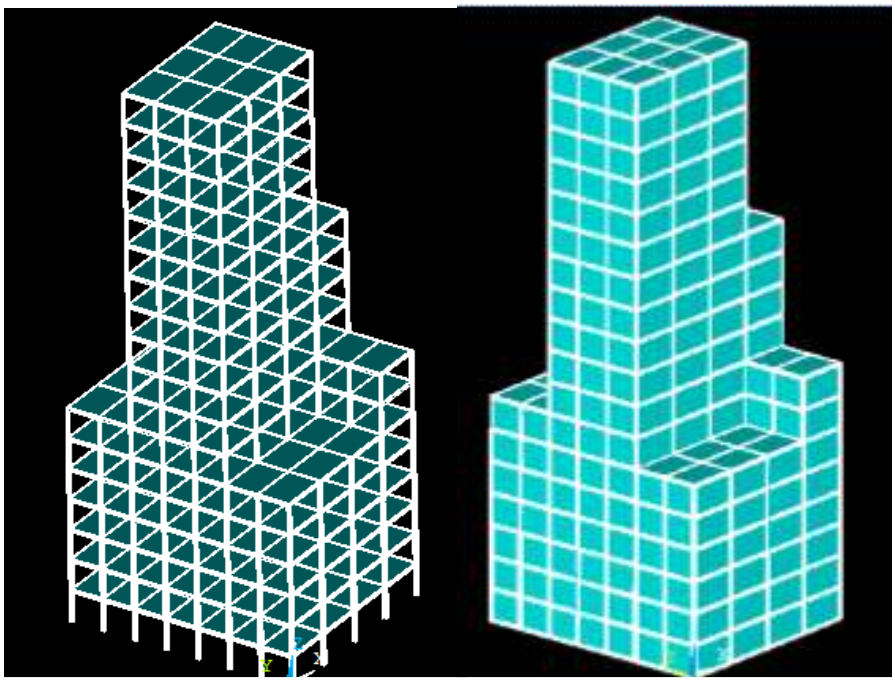

(a) (b)

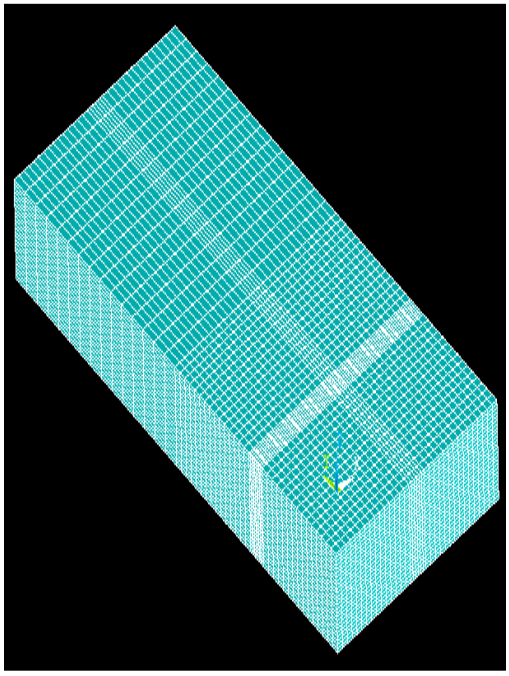

(c)

Fig. 3. Structural and fluid domain in ANSYS: (a) Beam steel structure and slabs of reinforced concrete. (b) Side covers of building. (c) Fluid domain enveloping the building

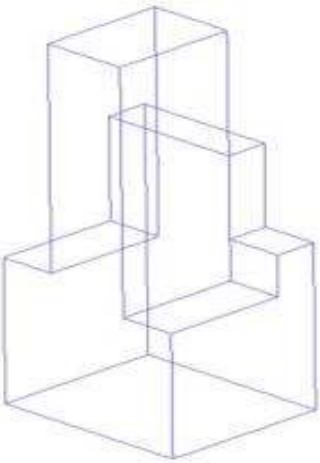

(a)

(b)

Fig. 4. Structural and fluid domain in Dines + GiD:
(a) Building as a rigid body. (b) Fluid Domain around the building

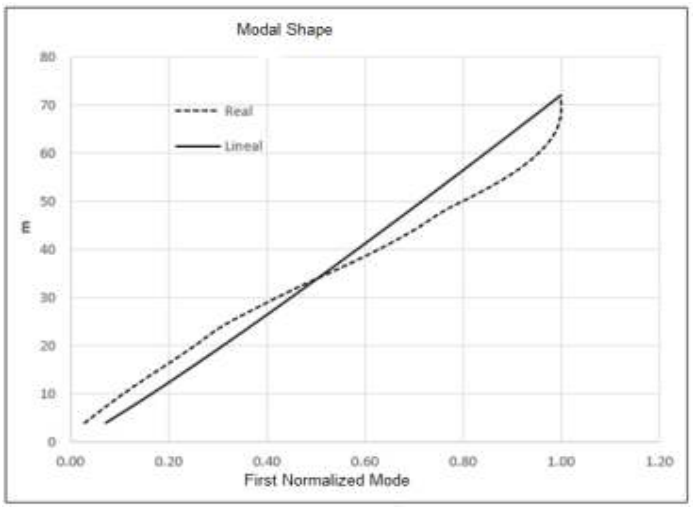

Fig. 5. Mode Shape of Prototype

Fig. 6. Scale model made of PVC foamed material

Fig. 7. Wind tunnel and instrumented scale model

Fig. 8. Equipment used on test measurements

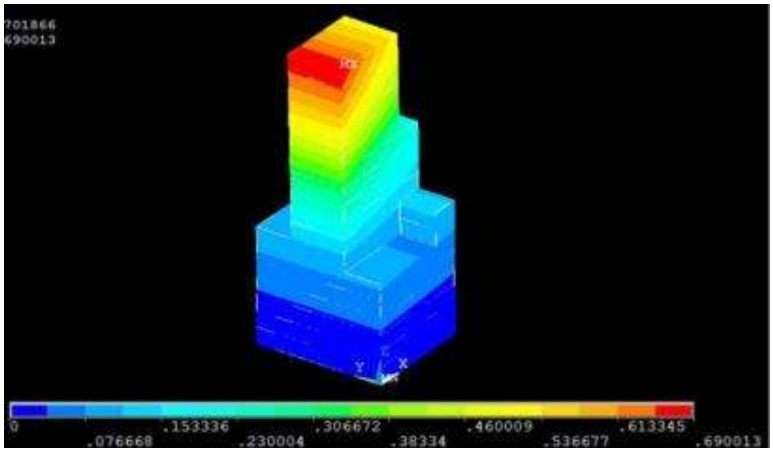

Fig. 9. Displacement results for t=1.0 sec

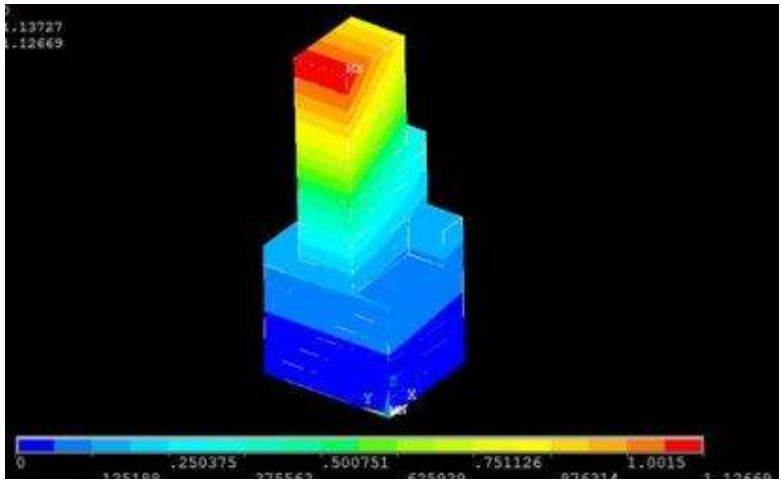

Fig. 10. Displacement results for t=1.1 sec

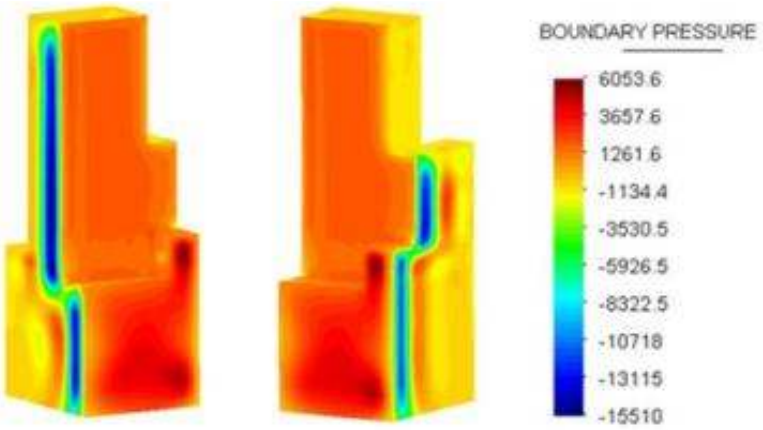

Fig. 11. Pressure contours for a time t=1.0 sec

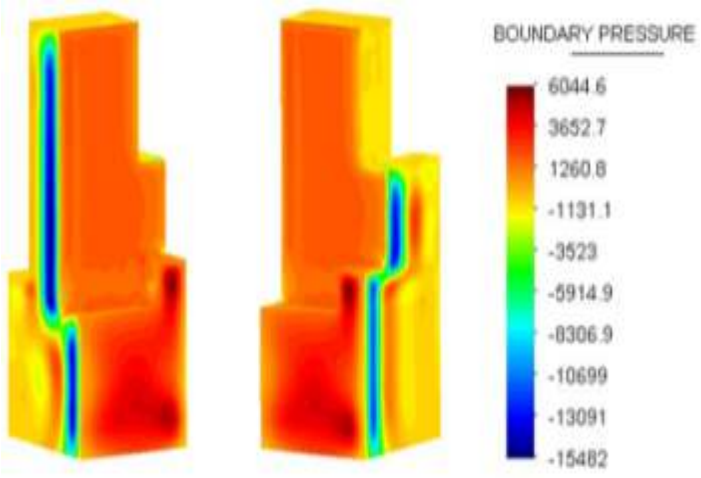

Fig. 12. Pressure contours for a time t=1.3 sec

The test in the wind tunnel allows us to compare results with those obtained from computational modeling. Regarding DINES + GiD software, here it is only possible to compare the maximum moment obtained with respect to the wind tunnel. On the other hand ANSYS solutions allow as compare displacement and moment at the basement. We proceed to make a comparison (value: e) between experimental obtained results with respect to the computational modeling.

$$e = \frac{55.4 - 47.5}{55.4} = 0.142 = 14.2\ \%\ \text{using ANSYS}$$

$$e = \frac{55.4 - 53.7}{55.4} = 0.031 = 3.1\ \%\ \ \text{using DINES + GiD}$$

4. CONCLUSIONS

The above results observe differences in part by the different algorithms applied on each program. Some remarks resulting from this work are as follow:

The physical scale model used in this work is quite similar to that shown in Ansys, which is in turn based on the twist that occurs in the basement of the model due to the wind effect, so, the physical model behaves like a rigid body. On the other hand the torsion effect it was not considered in our scale model, but from ANSYS Simulation it is observed to be significant the torsion effect in the highest points of the structure.

In Dines + GiD, the structural model is considered as a rigid body fixed at the basement, so it has been possible to run the wind algorithm turbulently because a quantity of finite elements within the fluid domain were enough to achieve the corresponding convergence criterion, this number of elements was possible due to the no transfer process of pressure towards another domain.

In ANSYS both domains were modeled, but in the flow domain fewer elements were used due to the fact that was proposed that only the fluid pressure on the external nodes of the tridimensional frame structure will be transferred, this proposal was suggested because it was no possible introduce real material properties of plates cover glasses, in another case, this plates will be highly deformed causing early failures. ANSYS algorithm requires a structural surface to be adjacent to the fluid domain to calculate the displacement in the boundary between domains, because of this, was not possible to propose a finer mesh to achieve convergence criteria in a turbulent fluid model and therefore it was chosen a laminar flow.

Despite the large numerical and experimental development nowadays, difficulties prevail for solving this kind of structures having a complex geometry. This work can be useful in choosing criteria for analogous analysis cases of high buildings subject to wind effects.

COMPETING INTERESTS

Authors have declared that no competing interests exist.

REFERENCES

1. Breuer M, De Nayer G, Münsch M, Gallinger T, Wüchner R. Fluid-structure

interaction using a partitioned semi-implicit predictor-corrector coupling scheme for the application of large-eddy simulation. Journal of fluids and Structures. 2012;29: 107-130

2. Wood C, Gil AJ, Hassan O, Bonet J. Partitioned block-Gauss-Seidel coupling for dynamic fluid-structure interaction. Computers and Structures. 2010;88:1367-1382.
3. Huerta A, Sarrate J, Donea J. Arbitrary Lagrangian-Eulerian formulation for fluid-rigid body interaction. Comput. Methods Appl. Mech. Engrg. 2001;190:3171-3188.
4. Drinkler D, Hübner B, Walhorn E. A monolithic approach to fluid-structure interaction. Comput. Methods Appl. Mech. Engrg. 2004;193:2087-2104.
5. Valdés-Vázquez JG. Nonlinear analysis of orthotropic membrane and shell structures including fluid-structure interaction. PhD Thesis, Universitat Politecnica de Catalunya, España; 2007.
6. Belver AV, Ibán AL, Lavín-Martín CE. Coupling between structural and fluid dynamic problems applied to vortex shedding in a 90 m steel chimney. J. Wind Eng. Ind. Aerodyn. 2012;100:30-37.
7. Matthies HG, Niekamp R, Steindorf J. Algorithms for strong coupling procedures. Comput. Methods appl. Mech. Engrg. 2006;195:2028-2049.
8. Masud A, Khurram RA. 2006. A multiscale/stabilized formulation of the incompressible Navier-Stokes equations for moving boundary flows and fluid-structure interaction. Comput. Mech. 38, 403-416.
9. Richter T, Wick T. Finite elements for fluid-structure interaction in ALE and fully Eulerian coordinates. Comput. Methods Appl. Mech. Engrg. 2010;199:2633-2642.
10. Wall WA, Genkinger S, Ramm E. A strong coupling partitioned approach for fluid-structure interaction with free surfaces. Computers & Fluids. 2007;36:169-183.
11. Tezduyar TE, Sathe S, Keedy R, Stein K. Space-time finite element techniques for computation of fluid-structure interactions. Comput. Methods Appl. Mech. Engrg. 2006;195:2002-2027.
12. Zhang Q, Zhu B. An integrated coupling framework for highly nonlinear fluid-structure problems. Computers & Fluids. 2012;60:36-48.
13. Zhou Y, Kareem A. Aeroelastic balance. Journal of Engineering Mechanics. 2003; 129:283-292.
14. Gurtin ME. An introduction to continuum mechanics. Academic Press; 1981.
15. Slone AK, Pericleous K, Bailey C, Cross M. Dynamic fluid-structure mesh procedures. Computers and Structures. 2002;80:371-390.
16. Cook RD. Finite element modeling for stress analyses. Wiley; 1995.
17. Bathe KJ, Baig MMI. On a composite implicit time integration procedure for nonlinear dynamics. Computers and Structures. 2005;83:2513-2524.
18. Peric D, Dettmer W. An analysis of the time integration algorithms for the finite element solutions of incompressible Navier-Stokes equations based on a stabilized formulation. Comput. Methods Appl. Mech. Engrg. 2003;192:1177-1226.
19. Fries TP, Matthies HG. A stabilized and coupled meshfree / meshbase method for the incompressible Navier-Stokes equations-Part I: Stabilization. Comput. Methods Appl. Mech. Engrg. 2006;195: 6205-6224.
20. Codina R, Soto O. Approximation of the incompressible Navier-Stokes equations using orthogonal subscale stabilization and pressure segregation on anisotropic finite element meshes. Comput. Methods Appl. Mech. Engrg. 2004;193:1403-1419.
21. Badia S, Codina R. Fluid-structure iterative algorithms using pressure segregation methods and their application to bridge aerodynamics. In: P. Wesseling, E. Oñate, J. Periaux (Eds.) European Conference on Computational Fluid Dynamics. Netherlands; 2006.
22. Ponthot JP, Belytschko T. Arbitrary Lagrangian-Eulerian formulation for element-free Galerkin method. Comput. Methods Appl. Mech. Engrg. 1998;152:19-46.
23. Wick T. Fluid-structure interactions using different mesh motion techniques. Computers and Structures. 2011;89:1456-1467.
24. Borst R, Kuhl E, Hulshoff S. An arbitrary Lagrangian Eulerian finite-element approach for fluid-structure interaction phenomena. Int. J. Numer. Meth. Engrg. 2003;57:117-142.
25. Matthies HG, Steindorf J. Partitioned but strongly coupled iteration schemes for nonlinear fluid-structure interaction.

Computers and Structures. 2002;80:1991-1999.
26. Boggs DW. Validation of the aerodynamic model method. Journal of Wind Engineering and Industrial Aerodynamics. 1992;41-44:1011-1022.
27. ASCE Standards; 2012.
28. Craig Jr. RR. Structural dynamics. Wiley; 1981.
29. ANSYS Inc. Software. Versión 14.0; 2011.
30. DINES 2007. Algoritmo numérico para interacción fluido-estructura. Jesús Gerardo Valdés Vázquez. Universidad de Guanajuato, México.
31. GiD. Software for pre-process and post-process of the finite element method. R. Ribo, M. Pasenau, E. Escolano, J. Suit, y A. Coll. CIMNE, Barcelona; 2007.

Peer-review history:
The peer review history for this paper can be accessed here:
http://sciencedomain.org/review-history/12417